DOI: 10.26599/FSHW.2026.9251185

Contents lists available at SciOpen

Food Science and Human Wellness

journal homepage: https://www.sciopen.com/journal/2097-0765

China Food Publishing Co.

Targeting uropathogenic *Escherichia coli* virulence: peanut skin extract as a potential non-antibiotic strategy for Urinary tract infection prevention

Mo Zhang [ab], Daiyuan Zhang [ab], Qun Lu [abc], Mingjuan Xu [ad], Cheng Lv, [ad], Lili Pang [ab], Rui Liu [abce]*

[a] *College of Food Science and Technology, Huazhong Agricultural University, Wu Han 430000, China*

[b] *Key Laboratory of Environment Correlative Dietology (Huazhong Agricultural University), Ministry of education, Wu Han 430000, China*

[c] *Wuhan Engineering Research Center of Bee Products on Quality and Safety Control, Wu Han 430000, China*

[d] *School of Public Health, Hubei University of Medicine, Shiyan 442000, China*

[e] *Key Laboratory of Urban Agriculture in Central China, Ministry of Agriculture and Rural Affairs, Wu Han 430000, China*

ABSTRACT: Urinary tract infections (UTI), predominantly caused by uropathogenic *Escherichia coli* (UPEC), represent a significant global health burden, exacerbated by the rising challenge of antibiotic resistance. Peanut skin extract (PSE), a procyanidin-rich extract with abundant A-type linkages, exhibits anti-UPEC activity. However, its high MIC (10 mg/mL) suggests a predominant anti-virulence mechanism rather than direct bactericidal action. To test this, we evaluated the impact of PSE at sub-inhibitory concentrations (≤1000 μg/mL) on critical UPEC virulence factors. PSE significantly inhibited UPEC motility by downregulating flagella-associated genes (*fliC, flhC,* and *flhD*). Adhesion and invasion assays using T24 bladder epithelial cells and Caco-2 intestinal epithelial cells demonstrated PSE's ability to reduce UPEC colonization, likely due to suppressed expression of fimbrial assembly genes (*fimC, fimH, papC,* and *papG*). Importantly, PSE disrupted biofilm formation, as evidenced by reduced biofilm mass and downregulation of the biofilm-associated *flu* gene. In addition, further protein level analysis confirmed a significant reduction in the expression of key virulence factors, including FlhD, FimH, and Ag43. Using a mouse UTI model, PSE intervention reduced bacterial colonization in the bladder and alleviated inflammation, aligning with *in vitro* findings. These results suggest that PSE mitigates UPEC pathogenicity by targeting virulence factors, offering a promising complementary approach for managing UTI and reducing reliance on antibiotics.

Keywords: Urinary tract infections; Peanut skin extract, Uropathogenic *Escherichia coli*, Virulence factors, Alternative antimicrobial strategies.

1. Introduction

Urinary tract infections (UTI) are among the most prevalent bacterial infections worldwide, with an estimated global incidence of 150–250 million cases annually [1]. In the United States alone, the annual economic burden of UTI exceeds USD 6 billion [2]. If left untreated, UTI may progress to severe complications, including pyelonephritis, renal failure, and sepsis [3]. Uropathogenic *Escherichia coli* (UPEC), which originates from the intestinal tract, is responsible for approximately 80% of UTI. After ascending to the urinary tract, UPEC adheres to the bladder epithelium and initiates infection [4-6]. Its pathogenicity is largely

***Corresponding author**
liurui@mail.hzau.edu.cn (R. Liu)

Received 3 July 2025
Received in revised from 22 January 2026
Accepted 11 February 2026

mediated by several virulence factors, including type 1 and P fimbriae, which promote adhesion to host epithelial cells and enable resistance to urinary flow [3, 7]. In addition, flagella contribute to motility and facilitate tissue invasion [8]. UPEC is also capable of forming biofilms, which not only shield bacteria from immune responses but also reduce antibiotic penetration by forming a physical barrier, thereby exacerbating resistance [9]. Although antibiotics remain the primary treatment for UTI, the widespread use of these drugs has led to the emergence of antibiotic resistance. According to the World Health Organization (WHO), UPEC has demonstrated increasing resistance to commonly used antibiotics, such as fluoroquinolones, cephalosporins, and sulfonamides [10]. The rise of multidrug-resistant strains has significantly compromised the clinical efficacy of first-line treatments. Moreover, antibiotic therapy is frequently associated with adverse effects, such as gut microbiota dysbiosis, allergic reactions, and an increased risk of recurrent infections due to incomplete eradication of virulence factors [11, 12]. In addition, the overuse of antibiotics exerts strong selective pressure, accelerating the emergence of multidrug-resistant UPEC strains [13]. These limitations highlight the urgent need for alternative approaches that can mitigate UPEC pathogenicity without contributing to resistance development.

Natural bioactive compounds have received increasing attention as potential alternatives to conventional antibiotics due to their low toxicity, broad availability, and favorable biocompatibility. Peanut skin, a byproduct of peanut processing, accounts for approximately 2.6% of the total peanut weight [14]. Owing to its coarse texture and astringent taste, it has traditionally been regarded as a low-value material, often used as animal feed or fuel. Recent pharmacological studies have shown that peanut skin is a rich source of plant polyphenols, especially procyanidins (PACs), which are considered the main contributors to its biological activity. PACs are secondary metabolites composed of catechin or epicatechin units.

Several studies have shown that plant-derived polyphenols, including PACs, can inhibit bacterial growth through multiple mechanisms [15]. For instance, procyanidin-rich grape seed extract have been reported to disrupt the integrity and permeability of bacterial membranes, leading to the leakage of intracellular contents and disruption of cellular homeostasis [16, 17].

Traditional antimicrobial approaches primarily focus on bacterial killing or growth inhibition. However, these strategies can accelerate the development of antibiotic resistance and cause collateral damage to the host microbiota [18]. It is important to note that the pathogenicity of UPEC is more dependent on virulence factors such as fimbrial adhesion, flagellar motility, and biofilm formation, rather than on its replication capacity alone. Therefore, increasing attention has been given to anti-virulence strategies, which aim to suppress bacterial pathogenic mechanisms without exerting bactericidal pressure [19]. This approach may reduce host tissue damage and mitigate the selection pressure that drives resistance. For UPEC-related UTI, anti-virulence interventions hold promise. Inhibiting fimbriae-mediated adhesion may prevent UPEC colonization of the urinary epithelium and thereby block the initial stages of infection [20]. Similarly, preventing biofilm formation may enhance bacterial clearance by host defenses and antibiotics, reducing the likelihood of recurrence [21]. In this context, PACs have shown potential in targeting multiple UPEC virulence mechanisms. Previous studies

have reported that PACs can downregulate the expression of fimbrial genes, thereby impairing UPEC adhesion and invasion of epithelial cells [22, 23]. By interfering with the specific interaction between UPEC and host cells, this mechanism may reduce the risk of resistance development.

Although an increasing number of studies support the anti-virulence potential of PACs, most current research remains limited to *in vitro* models and tends to focus on single pathogenic traits. Comprehensive analyses of their effects on multiple pathogenic traits remain limited. Based on the nature of interflavan linkages, PACs are typically classified into A-type and B-type. Some studies, particularly those examining cranberry-derived PACs, suggest that their high content of type A structures may exhibit stronger anti-adhesion or antiviral activity against urinary tract pathogens [24]. By comparison, our previous compositional analysis showed that procyanidins account for up to 85.69% of PSE [25]. The PACs in PSE are mainly composed of low degree A type oligomers, including various type A dimers and type A trimers. Together, these features indicate that PSE represents a composite polyphenolic system dominated by low-oligomeric procyanidins. Based on this, we further explored the potential of PSE to attenuate the pathogenicity of UPEC.

In this study, we investigated the anti-virulence effects of PSE, rich in A-type PACs, on UPEC. Both *in vitro* assays and a murine UTI model were employed to evaluate its influence on key virulence determinants, including motility, epithelial adhesion and invasion, and biofilm formation. These findings provide mechanistic insights into the anti-pathogenic potential of PSE and support its application as a natural, non-antibiotic strategy for the prevention and management of UTI. Given the growing limitations of conventional antibiotic therapies, PSE represents a promising alternative that targets bacterial virulence rather than viability, thereby reducing the selective pressure for resistance while preserving host microbiota.

2. Materials and methods

2.1 Bacterial strains

The UPEC strain CFT073 (ATCC 700928), originally isolated from the blood and urine of a patient with acute pyelonephritis in Baltimore, Maryland, was generously provided by Prof. Tan (Huazhong Agricultural University, China). The bacteria were revived from frozen stocks by streaking onto Luria-Bertani (LB) agar plates and incubated at 37°C for 24–48 hours.

2.2 PSE extraction and characterization

PSE was prepared as described previously [25]. Briefly, peanut skins were extracted with 70% ethanol (v/v) at 80°C for 90 minutes. The extract was centrifuged at 3,000 × g for 20 minutes, filtered, and concentrated at 38°C using a rotary evaporator to remove ethanol. The resulting product was purified using AB-8 macroporous resin with 40% ethanol as the eluent. Purified PSE was concentrated, frozen, and lyophilized for storage.

The composition of PSE was determined using reversed-phase high-performance liquid chromatography (RP-HPLC), based on the method established by Zhao [25]. In brief, PSE was dissolved in methanol, filtered

through a 0.22 μm membrane, and injected into a Hypersil GOLD C18 column (250 × 4.6 mm, 5 μm). Separation was performed at 30°C with a 10 μL injection volume and a flow rate of 0.8 mL/min using a gradient elution: 0–10 min, 5% acetonitrile (B); 10–40 min, 5%–15% B; 40–80 min, 15%–40% B; 80–81 min, 40%–5% B; 81–90 min, 5% B. Detection was set at 280 nm.

2.3 Cell culture and treatments

The T24 human bladder epithelial cell line (ATCC HTB-4) was used due to its relevance in UTI studies. Cells were cultured in RPMI-1640 medium supplemented with 10% fetal bovine serum at 37°C in a humidified 5% CO_2 atmosphere. For experiments, 1 × 10^4 cells were seeded into 96-well plates and maintained until approximately 90% confluence, with media refreshed every other day. Caco-2 human intestinal epithelial cells were cultured in high-glucose DMEM supplemented with 15% fetal bovine serum and 1% penicillin–streptomycin at 37°C in a humidified incubator with 5% CO_2.

2.4 Minimum inhibitory concentration (MIC) and bacterial growth inhibition

The MIC of PSE against UPEC was determined using the broth microdilution method, following the protocol described by Wiegand et al. [26]. To confirm MIC results, gradient-diluted bacterial suspensions were spot-inoculated in equal volumes onto LB agar plates. Additionally, bacterial growth dynamics were evaluated by inoculating log-phase UPEC into LB broth containing varying concentrations of PSE. Cultures were incubated at 37°C with shaking (140 rpm), and optical density at 600 nm (OD_{600}) was recorded at designated time points (0, 2, 4, 6, 12, and 24 hours) (Yep et al., 2014).

2.5 Bacterial motility assays

Swimming and swarming abilities were assessed following the method described in previous studies [27]. Semi-solid agar plates were prepared with swimming medium or swarming medium, supplemented with varying concentrations of PSE. 3 μL bacterial suspension was inoculated at the center of each plate, followed by incubation at 37°C for 24 hours. The diameters of motility zones were measured to assess motility inhibition.

2.6 Adhesion and invasion assays

Adhesion and invasion assays were performed according to previously published methods, with slight modifications [28]. Log-phase UPEC was pre-treated with PSE at various concentrations for 2 hours, then resuspended in serum-and antibiotic-free RPMI-1640 medium. T24 cells were infected at a multiplicity of infection of 100 for 2 hours. Non-adherent bacteria were removed by washing, and adherent bacteria were quantified by plating after trypsinization. For invasion assays, extracellular bacteria were eliminated by gentamicin treatment prior to cell lysis and intracellular bacterial quantification. Inhibition rates were calculated relative to untreated controls.

Adhesion and invasion assays were performed according to previously published methods, with minor modifications.

2.7 Bacterial ultrastructure by TEM

PSE intervention treatments (control group and 500 μg/mL group) for UPEC were consistent with 2.6. Then, UPEC were fixed with 2.5% glutaraldehyde and stained with 3% molybdate. Samples were visualized under a transmission electron microscope (Hitachi-7800, Tokyo, Tokyo Met, Japan) to examine bacterial surface structures, including fimbriae and flagella.

2.8 Biofilm quantification and microscopic visualization

Biofilm formation was assessed by incubating UPEC cultures (adjusted to 10^7 CFU/mL) with PSE in 96-well plates at 37°C for 24 hours. After removing non-adherent bacteria by PBS washing, biofilms were stained with crystal violet and quantified by measuring absorbance at 570 nm following ethanol solubilization [29]. For microscopic observation, biofilms formed in 24-well plates were stained with 50 μg/mL fluorescein isothiocyanate-conjugated concanavalin A (FITC-Con A; Sigma, St. Louis, MO, USA), a fluorescent probe targeting extracellular polysaccharides, and visualized under a fluorescence microscope [30].

2.9 Gene and protein expression analysis

Intervention treatment for bacteria as in 2.6. RNA in CFT073 was extracted, reverse transcribed and quantified using the relevant kit (ABclonal, Wuhan, China) [14]. The standard curve method and Software (version 4.3.1.0) (Analytic jena, German) were used for data analysis. Relative expression of the target gene was calculated using $2^{-\Delta\Delta Ct}$ methods. Specific primers used for RT-qPCR are shown in Table 2.

Table 2 Sequence of the primers used in this study.

Gene	Forward primer (5'-3')	Reverse primer (5'-3')
16S rRNA	GGCGCATACAAAGAGAAG	ATGGAGTCGAGTTGCAGA
fliC	ACAGCCTCTCGCTGATCACTCAAA	GCGCTGTTAATACGCAAGCCAGAA
flhC	CATGCTGCCATTCTCAACCG	TTGCGGGCACTGTTCAAGGT
flhD	TGCATACCTCCGAGTTGCTG	CCGAGACGAAACATAGCGGA
fimC	CTAAATTAGCGTTGCCACCCG	AGGGTGTCGGGTTAATCAGC
fimH	GTGCCGATTCCTCTTACCGTT	TGGAATAATCGTACCGTTGCG
papC	GTGGCAGTATGAGTAATGACCGTTA	ATATCCTTTCTGCAGGGATGCAATA
papG	GACTGAGAAATTTAACGATATTATTTT	CACATTGTATGGGATTTTAAAACG
flu	TAACAGCGTCCGTCTCAGCATTCA	AACATCAACGGAAGAATGGCCTGC

The treatment of UPEC strains by PSE is as described in Section 2.6. Bacterial cells were lysed using RIPA lysis buffer, and total protein concentration was determined with a BCA protein assay kit. Equal amounts of protein (10 μg) were separated by 12% SDS-PAGE and transferred onto 0.22 μm polyvinylidene fluoride (PVDF) membranes. The membranes were blocked with 5% skim milk at room temperature for 2 h and then incubated overnight at 4°C with the following primary antibodies: FlhD (1:1000), FimH (1:1000), Ag43 (1:1000), and GAPDH (1:2000). After incubation with HRP-conjugated secondary antibodies at room temperature, protein bands were visualized using an enhanced chemiluminescence detection kit. Band intensities were quantified using ImageJ software and normalized to GAPDH.

2.10 Mouse Model of UPEC Infection

Female C57BL/6 mice (6–8 weeks old) were obtained from the Laboratory Animal Center of Huazhong Agricultural University and housed under specific pathogen-free conditions (12 ± 1 h light/dark cycle, 20 ± 2°C, 50%–60% relative humidity) with ad libitum access to food and water. All procedures complied with the

National Guidelines for the Use of Experimental Animals (China) and the Huazhong Agricultural University Animal Care Guidelines, and were approved by the Huazhong Agricultural University Animal Ethics Committee (Approval No.HZAUMO-2024-0059). The animal qualification certificate number is No. 42816300016019. The Laboratory Animal Center of Huazhong Agricultural University is licensed for animal use (License No. SYXK(E) 2020-0084). After one week of acclimatization, the mice were randomly assigned into three groups (n = 4/group).

The UTI model was established with slight modifications based on previous studies [31]. UPEC strains treated with PSE (as described in Section 2.6) were resuspended in sterile PBS. Mice were anesthetized with isoflurane, and residual urine was expelled by gentle abdominal pressure. A sterile catheter-sheathed syringe was inserted transurethrally to instill 50 μL of bacterial suspension into the bladder. After 24 h, mice were weighed and euthanized. Bladders were aseptically excised, rinsed to remove residual urine, and weighed to calculate the bladder index (bladder weight (mg)/body weight (g)). Morphological and pathological changes were recorded. The bladder was divided into two parts. One part was fixed overnight in 4% paraformaldehyde at 4°C. After fixation, tissue sections were deparaffinized, rehydrated, and stained with hematoxylin and eosin (H&E) following standard protocols. Morphological and pathological changes, including inflammation and tissue damage, were evaluated under a light microscope, and representative images were captured for further analysis. The other part was homogenized in sterile PBS, and bacterial load was quantified by plating, expressed as CFU per mg of tissue. Supernatants from homogenates (5,000 × g, 10 min, 4°C) were collected for cytokine analysis. IL-6 and TNF-α levels were measured using ELISA kits (ABclonal, Wuhan, China).

2.11 Statistical analysis

All experiments were performed in triplicates and the data was expressed as mean ± standard deviation (SD). Statistical analysis was performed by one-way analysis of variance (ANOVA) using SPSS software (version18.0). Differences at $P < 0.05$ were considered statistically significant.

3. Results and discussion

3.1 Determination of procyanidin content in PSE and characterization of PSE.

Peanut skin is a rich source of polyphenolic compounds, especially procyanidins. The composition of PSE was characterized by comparing their high-performance liquid chromatography (HPLC) profiles with those from our previous findings [25]. As shown in Fig. 1A and summarized in Table 1, PSE is abundant in procyanidins, predominantly featuring A-type interflavan linkages. A-type procyanidins are known to possess stronger antibacterial and anti-adhesive properties than their B-type counterparts, especially against *Escherichia coli* [32]. The high content of A-type procyanidins in PSE may contribute to its ability to significantly reduce bacterial adhesion and invasion in UTI models.

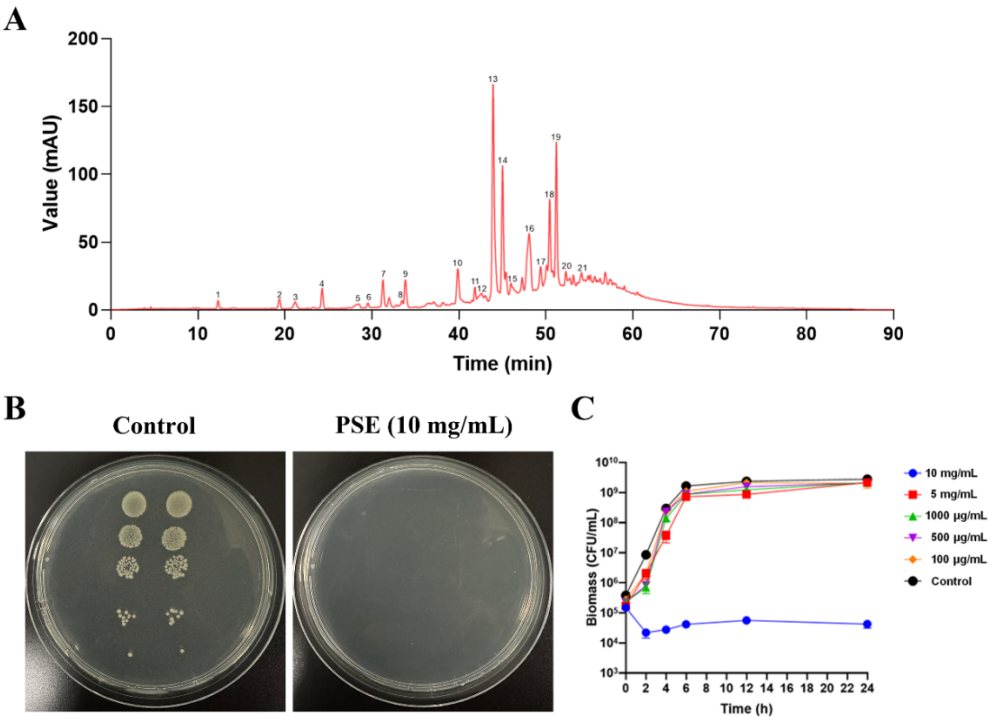

Fig. 1. Liquid chromatogram (A) of PSE and its MIC (B) and growth inhibition curve (C) for UPEC. Each value represents the average of three reproducible experiments. Bars represent the standard deviation (n = 3).

Table 1 Identification of PSE by HPLC based on retention time.

Peak	RT (min)	Tentative Identification
1	12.33	unknown
2	19.37	unknown
3	21.19	Procyanidin dimer B-type
4	24.29	(+)-Catechin
5	28.51	Procyanidin dimer B-type
6	29.56	Procyanidinte tramer A-type
7	31.28	Procyanidin trimer A-type
8	33.46	(-)-Epicatechin
9	33.86	Procyanidin trimer A-type
10	39.89	Procyanidin tetramer 2 A-type linkages
11	41.85	Procyanidin dimer B-type
12	42.61	Procyanidin tetramer A-type linkages
13	43.95	Procyanidin dimer A-type
14	45.03	Procyanidin trimer A-type
15	46.00	Procyanidin trimer A-type
16	48.08	Procyanidin tetramer 2 A-type linkages
17	49.40	Procyanidin tetramer 2 A-type linkages
18	50.45	Procyanidin dimer A-type
19	51.22	Procyanidin tetramer 2 A-type linkages
20	52.31	Procyanidin tetramer 2 A-type linkages
21	54.11	Procyanidin tetramer 2 A-type linkages

3.2 Inhibitory effect of PSE on the growth of UPEC.

UPEC is the primary pathogen responsible for UTI. Procyanidins, particularly type-A procyanidins, have been widely recognized for their antimicrobial potential through mechanisms such as disrupting bacterial membrane integrity and impairing essential physiological functions [33]. The antibacterial activity of PSE was evidenced by an MIC of 10 mg/mL, as supported by LB agar plate assays showing visible suppression of UPEC growth at this concentration (Fig. 1B). Growth curve analysis further confirmed that PSE at 10 mg/mL

completely inhibited UPEC growth after 24 hours of incubation. In contrast, PSE had no significant effect on bacterial growth at lower concentrations (5 mg/mL, 1000 μg/mL, 500 μg/mL, and 100 μg/mL) (Fig. 1C).

These findings suggest that PSE has a concentration-dependent antibacterial effect. Complete inhibition was observed only at or above 10 mg/mL, whereas concentrations below 5 mg/mL exhibited minimal to no antibacterial activity. This is consistent with previous findings reporting an MIC of 18 mg/mL for cranberry procyanidin extract against enteropathogenic *E. coli* [34]. Although PSE exhibits some direct antibacterial activity, its relatively high MIC suggests that its direct bactericidal effect is limited. Therefore, we hypothesize that its primary bioactivity lies in attenuating bacterial virulence rather than inhibiting bacterial growth. Supporting this, several studies have shown that many natural compounds can effectively suppress key virulence factors — such as adhesion, motility, and biofilm formation — at sub-MIC levels [35]. For example, rutin at sub-inhibitory concentrations significantly reduces the adhesion and biofilm formation of pathogenic bacteria, and allicin also reduces biofilm formation, adhesion, and motility of UPEC at sub-inhibitory concentrations [36, 37]. These findings suggest that plant-derived polyphenols may exert their anti-infection effects by targeting virulence factors rather than bacterial survival rates. Based on these results, PSE concentrations of 100 μg/mL, 500 μg/mL and 1000 μg/mL, corresponding to 1/100 MIC, 1/20 MIC and 1/10 MIC respectively, were selected for subsequent experiments to investigate anti-virulence effects under sub-inhibitory conditions.

3.3 Inhibitory effect of PSE on the motility of UPEC

Motility, including swimming and swarming, is a key virulence factor that enables UPEC to ascend the urinary tract and initiate infection. To assess the inhibitory effect of PSE on UPEC CFT073 motility, swimming and swarming zones were measured on LB semi-solid agar. As shown in Fig. 2, swimming motility was significantly inhibited by PSE in a dose-dependent manner, with the motility zone area reduced from 34.49 mm² in the control to 16.96, 6.55, and 2.05 mm² at 100, 500, and 1000 μg/mL PSE, respectively. Swarming motility followed a similar trend, decreasing from 3.49 mm² to 1.96, 1.10, and 0.83 mm² at the same concentrations. These reductions, ranging from 50%–94% in swimming and 44%–76% in swarming, clearly demonstrate a dose-dependent suppression of UPEC motility by PSE ($P < 0.05$). Several studies have shown that targeting the motility of uropathogenic bacteria can effectively inhibit their virulence. For instance, β-sitosterol glucoside (SG) from *Citrus* significantly reduced the swimming and swarming motility of *Escherichia coli* O157:H7, thereby attenuating its pathogenicity [38]. Similar findings have been supported by other studies, such as t-resveratrol and oxyresveratrol, which significantly reduced fimbriae production and swarming motility in UPEC [39]. In addition, carvacrol and thymol found in oregano and thyme have also been shown to significantly reduce the swarming motility of *Escherichia coli* at sub-inhibitory concentrations [40].

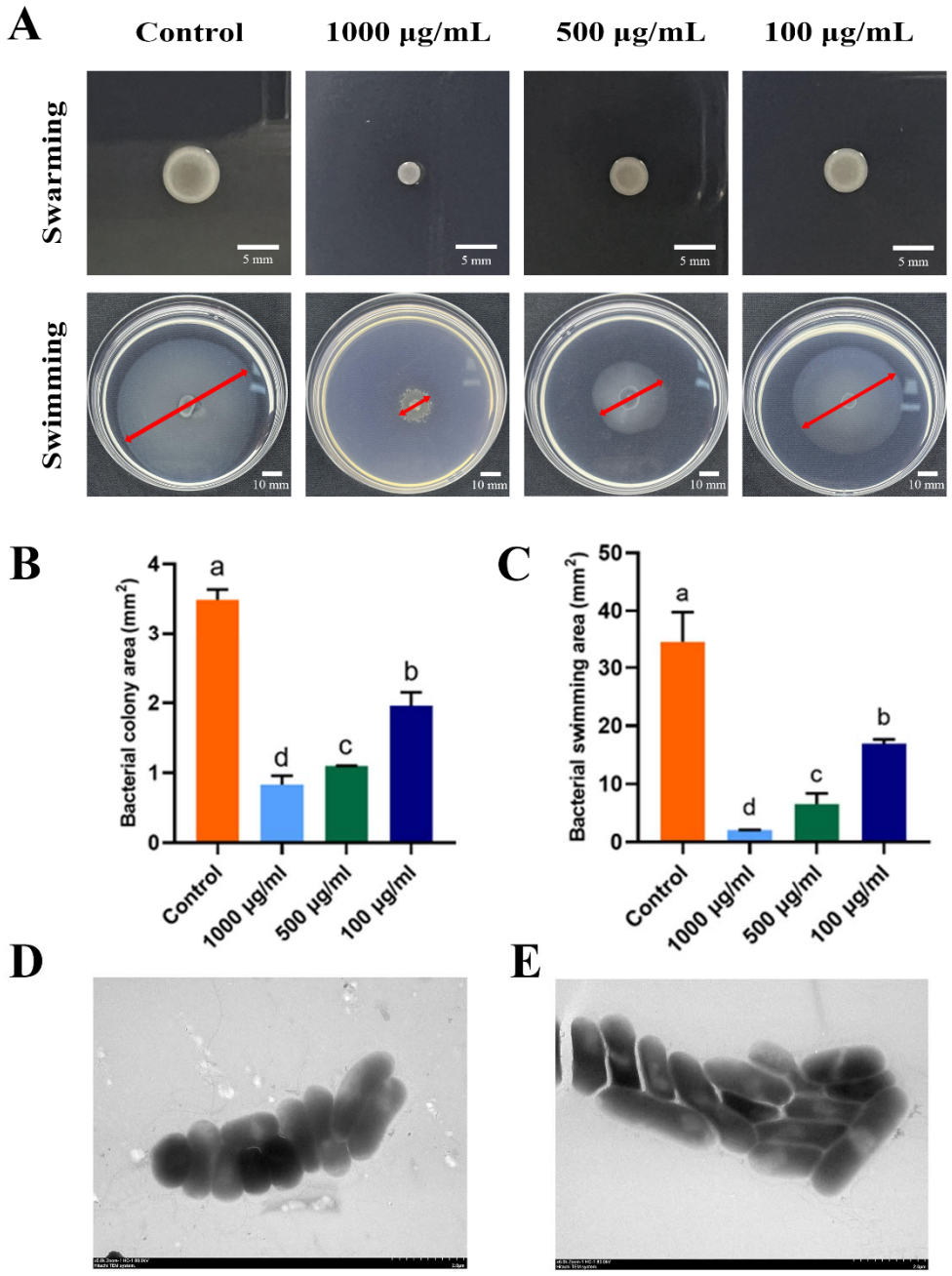

Fig. 2. PSE disrupted the flagellar structure of UPEC CFT073. The swarming (Scale bar = 5 mm) and swimming (Scale bar = 10 mm) motility of UPEC CFT073 in the plate with different concentrations of PSE (A). The zone of swarming was measured after 24 hours (B). The zone (red arrow indicates) of swimming was measured after 24 hours (C). TEM images of untreated UPEC (D) and UPEC treated with 500 μg/mL PSE (E). Data are presented as mean ± SEM of n = 4 independent experiments. Values with different superscript letters (a, b and c) were significantly different at $P < 0.05$.

To further investigate the potential mechanism underlying the impaired motility, we examined the structural changes of bacterial flagella using transmission electron microscopy (TEM). As shown in Fig. 2D, untreated UPEC cells exhibited numerous intact and relatively long flagella on their surface. In contrast, after treatment with 500 μg/mL PSE (Fig. 2E), the number of flagella was significantly reduced, and the remaining flagella were shorter. This morphological change suggests that PSE disrupts the assembly or stability of flagella. Lane et al. demonstrated that UPEC mutants lacking flagella exhibited significantly reduced colonization ability in a mouse urinary tract infection model [41]. Given the critical role of flagella in bacterial motility, this disruption would severely impair UPEC's ability to swim, swarm, and aggregate on host tissues

and abiotic surfaces, leading to the observed decrease in motility [42]. Consistent with our findings, several plant-derived compounds have also been shown to target bacterial flagella and inhibit bacterial motility. For example, allicin in garlic has been reported to alter flagellar morphology and inhibit bacterial motility [37]. Additionally, polysaccharides from *Vaccaria segetalis* have been shown to downregulate the expression of flagella-related regulatory genes, leading to reduced flagella synthesis and limited motility [43]. These studies collectively highlight the therapeutic potential of targeting bacterial flagella to mitigate motility-associated virulence.

In conclusion, our results indicate that PSE can significantly inhibit UPEC swimming and swarming motility in a concentration-dependent manner by targeting the flagella, providing a promising therapeutic strategy for combating UPEC virulence.

3.4 Effect of PSE on UPEC Adhesion, Invasion

The adhesion and invasion of UPEC on host epithelial cells are critical steps in the pathogenesis of UTI, as they enable bacterial colonization and the establishment of infection. Disruption of these processes is therefore regarded as an effective strategy for UTI prevention and treatment, and may represent a potential mechanism by which PSE exerts its protective effects [3, 21,44].

To evaluate the anti-virulence potential of PSE in disrupting UPEC adhesion and invasion, the UPEC strain CFT073 was pretreated with PSE (100, 500, and 1000 μg/mL) for 2 hours, followed by infection of T24 human bladder epithelial cells — a widely adopted *in vitro* model for studying UPEC-host interactions due to its relevance to urothelial physiology and consistent expression of key receptors [45]. As shown in Fig. 3A, PSE significantly suppressed bacterial adhesion in a concentration-dependent manner. Relative to the control group, adhesion rates declined to 94.20%, 82.35%, and 59.99% at 100, 500, and 1000 μg/mL, respectively. The reductions observed at 500 and 1000 μg/mL were statistically significant ($P < 0.05$), indicating a marked inhibition of UPEC attachment to host cells. A similar dose-dependent trend was observed in the invasion assay (Fig. 3B), in which extracellular bacteria were eliminated via gentamicin treatment post-infection. PSE pretreatment at 500 and 1000 μg/mL significantly reduced intracellular bacterial loads to 50.85% and 33.90% of control values, respectively ($P < 0.05$), corresponding to 2.0-fold and 3.0-fold reductions. In addition, the Caco-2 cell line was used to further assess the adhesion and invasion of UPEC following PSE treatment. Because UPEC commonly originates from the intestinal tract, Caco-2 cells have been employed in previous studies to evaluate UPEC adhesion and invasion properties relevant to early stages of infection [46]. The results showed that PSE treatment led to a concentration-dependent reduction in UPEC adhesion to Caco-2 cells (Fig. 3C). Compared with the control group, adhesion rates decreased to 94.81%, 87.43%, and 81.97% at PSE concentrations of 100, 500, and 1000 μg/mL, respectively, with the reduction observed at 1000 μg/mL reaching statistical significance ($P < 0.05$). A similar trend was observed in the invasion assay (Fig. 3D). Following PSE pretreatment, intracellular bacterial levels were reduced to 94.81%, 87.43%, and 81.97% of control values at the corresponding concentrations, and the decrease at 1000 μg/mL was statistically significant ($P < 0.05$).

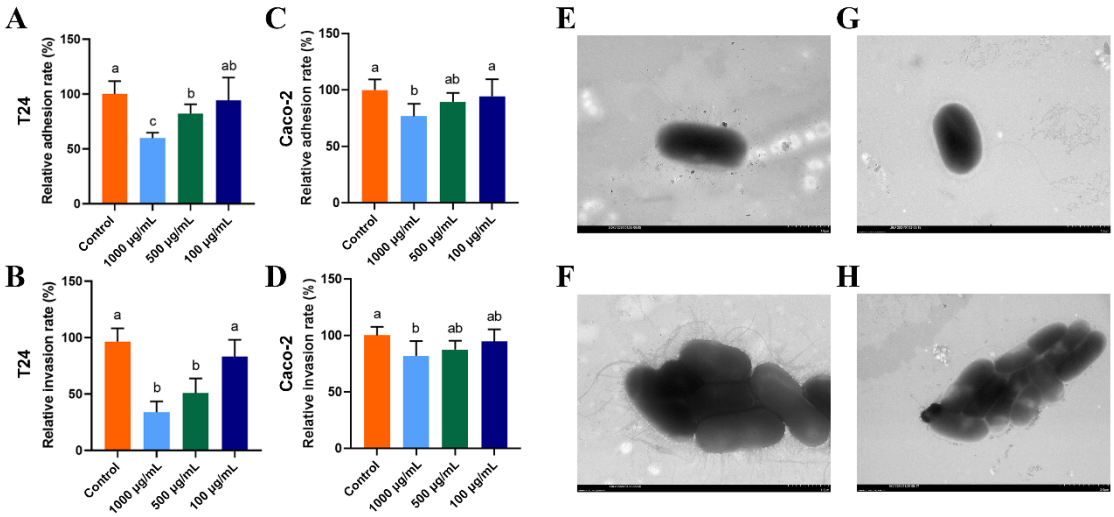

Fig. 3. PSE inhibits bacterial adhesion and invasion by reducing fimbrial abundance in UPEC. Relative adhesion (A) and invasion (B) rates of UPEC to T24 cells following treatment with different concentrations of PSE. Relative adhesion (C) and invasion (D) rates of UPEC to Caco-2 cells after PSE treatment. TEM images show untreated UPEC in individual (E) and clustered (F) states, and UPEC treated with 500 μg/mL PSE in individual (G) and clustered (H) states (scale bar = 1 μm). Data are presented as mean ± SEM from n = 4 independent experiments. Values with different superscript letters (a, b, and c) indicate statistically significant differences ($P < 0.05$).

These results collectively indicate that PSE inhibits UPEC adhesion and invasion in a concentration-dependent manner, thereby reducing its pathogenicity. Several studies have also intervened with pathogenic bacteria using similar approaches, demonstrating that extracts from *Betula pendula* (silver birch), *Urtica dioica* (nettle) and *Herniaria glabra* (glossy hawthorn) can reduce the hydrophobicity and motility of bacterial surfaces, thereby weakening the initial adhesion process and reducing the pathogenicity of the bacteria [47].

Fimbriae are the primary adhesion organelles of UPEC and are crucial for bacterial adhesion and colonization of the bladder epithelium [48]. Targeting fimbriae can effectively reduce bacterial virulence without inducing strong selective pressure for resistance, providing a promising strategy for antimicrobial therapy. To further investigate whether the observed adhesion and invasion dysfunctions are related to changes in fimbrial structure, we used transmission electron microscopy (TEM) to observe the morphological changes in fimbriae after PSE treatment. In the untreated control cells, dense and prominent fimbriae structures were clearly visible on the bacterial surface (Fig. 3E-F). In contrast, after treatment with PSE, especially at a concentration of 500 μg/mL, the fimbrial projections were significantly reduced, and the bacterial surface appeared much smoother (Fig. 3G-H). Given the critical role of UPEC fimbriae in the initial adhesion to host cells and subsequent invasion, the reduction in these structures is likely the underlying cause of the observed anti-adhesion and anti-invasion effects in the previous experiments [48]. This morphological evidence supports the hypothesis that PSE disrupts the assembly or stability of fimbriae, thereby weakening bacterial binding to host cells and establishing infection. This hypothesis has been reported in the literature. For example, polysaccharides from *Vaccaria segetalis* were shown to downregulate fimbrial gene expression in bacteria, thereby reducing bacterial contact and invasion [43]. Furthermore, dictamnine was also found to

inhibit the expression of type 1, P-type, and curli fimbrial genes in UPEC, reducing fimbriae numbers and consequently weakening its pathogenicity [49].

3.5 Effect of PSE on UPEC biofilm formation

Biofilm formation plays a pivotal role in the pathogenesis of UTI, enabling UPEC to adhere to surfaces, evade host immune responses, and resist antimicrobial treatment [21]. Following colonization of the urinary tract, UPEC readily develops biofilms that serve as persistent infection reservoirs and are closely associated with recurrent UTI [3]. Clinical studies have confirmed that UPEC isolates with high biofilm-forming capacity are more frequently associated with recurrent infections [50].

To investigate whether PSE could inhibit UPEC biofilm formation, we assessed its effect on strain CFT073 using crystal violet staining. As shown in Fig. 4A, PSE treatment resulted in a significant, dose-dependent reduction in biofilm biomass, with decreases of 21.48%, 36.56% and 54.29% at 100 μg/mL, 500 μg/mL and 1000 μg/mL, respectively ($P < 0.05$). Fluorescence microscopy using FITC-Con A further confirmed the disruption of biofilm architecture. While the untreated control group exhibited dense, continuous green fluorescence indicative of extensive biofilm development, treatment with PSE resulted in a marked reduction in biofilm surface coverage with increasing concentrations, and the biofilm structure appeared sparser and more fragmented. No fluorescence signal was observed in the blank group. Quantitative analysis of fluorescence-covered area revealed that PSE treatment significantly reduced biofilm surface coverage to 60.11%, 27.85% and 13.05% of the control level at 100 μg/mL, 500 μg/mL and 1000 μg/mL, respectively (Fig. 4C), demonstrating a pronounced inhibition of biofilm formation ($P < 0.05$). These results indicate that PSE effectively disrupts the formation and structural integrity of UPEC biofilms. Consistent with these findings, increasing evidence suggests that polyphenolic compounds from various plants exert anti-biofilm activity through multiple mechanisms. Tea polyphenols, resveratrol, and cranberry polyphenolic compounds have all been reported to inhibit biofilm formation by targeting bacterial adhesion, motility, and quorum sensing [17, 51, 52]. Although the mechanisms of action of these compounds differ, their common outcome is the disruption of biofilm establishment and maintenance. Furthermore, the anti-biofilm activity of PSE may also be attributed to its ability to interfere with early biofilm development events, particularly the initial adhesion and motility that are crucial for surface colonization and biofilm initiation. Research has found that luteolin, at sub-inhibitory concentrations, affected motility and fimbriae formation, which may be key mechanisms underlying its inhibition of biofilm formation [53]. Similarly, PSE may inhibit biofilm formation through similar mechanisms by regulating bacterial motility and fimbrial generation, further confirming its potential as an anti-biofilm agent.

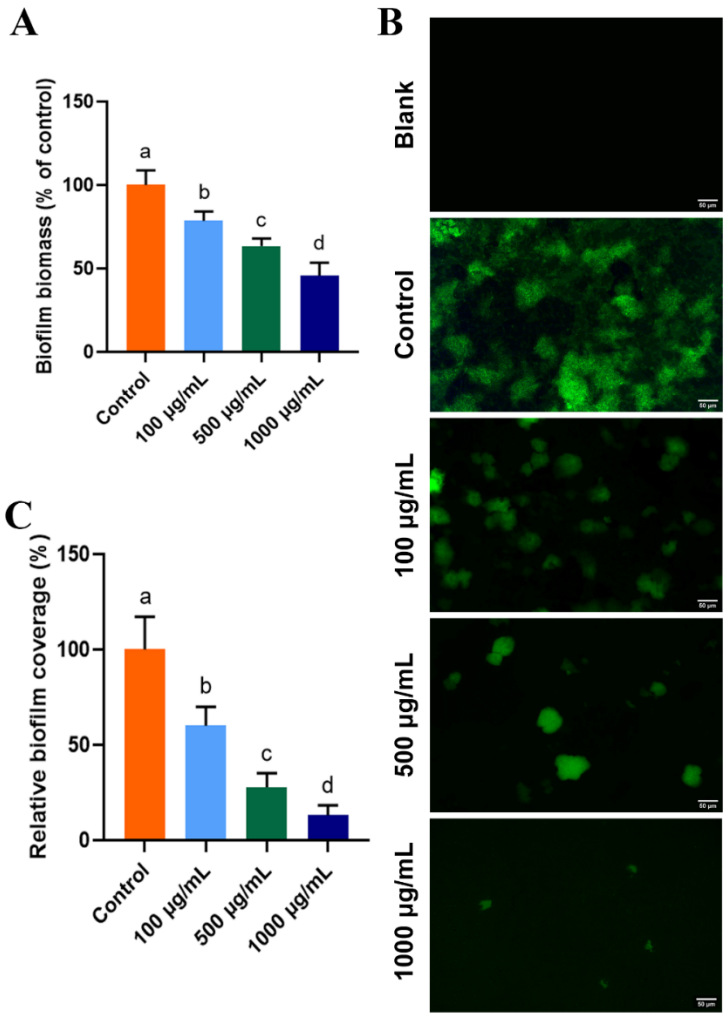

Fig. 4. The intervention of PSE significantly inhibited the formation of UPEC biofilm. Crystalline violet staining to assess biofilm formation at different concentrations of PSE (A). FITC-Con A fluorescence staining of UPEC biofilm formation after PSE 0 (Control), 100 μg/mL, 500 μg/mL, 1000 μg/mL intervention and aseptic group (Blank) (Scale bar = 50 μm) (B). Quantitative analysis of fluorescence-covered area was performed, with the control group normalized to 100% (C). Data are presented as mean ± SEM of n = 3 independent experiments. Values with different superscript letters (a, b and c) were significantly different at $P < 0.05$.

3.6 Effect of PSE on UPEC-related pathogenic genes

After characterizing the composition of PSE and its effects on UPEC virulence-related phenotypes, we next examined the underlying molecular mechanisms at the gene and protein levels. To obtain a comprehensive overview of the transcriptional response to PSE treatment, an expression heatmap of virulence-associated genes was generated (Fig. 5A), which revealed a downregulation of key genes involved in UPEC motility, adhesion, and biofilm formation, with more pronounced inhibition observed at the higher PSE concentration.

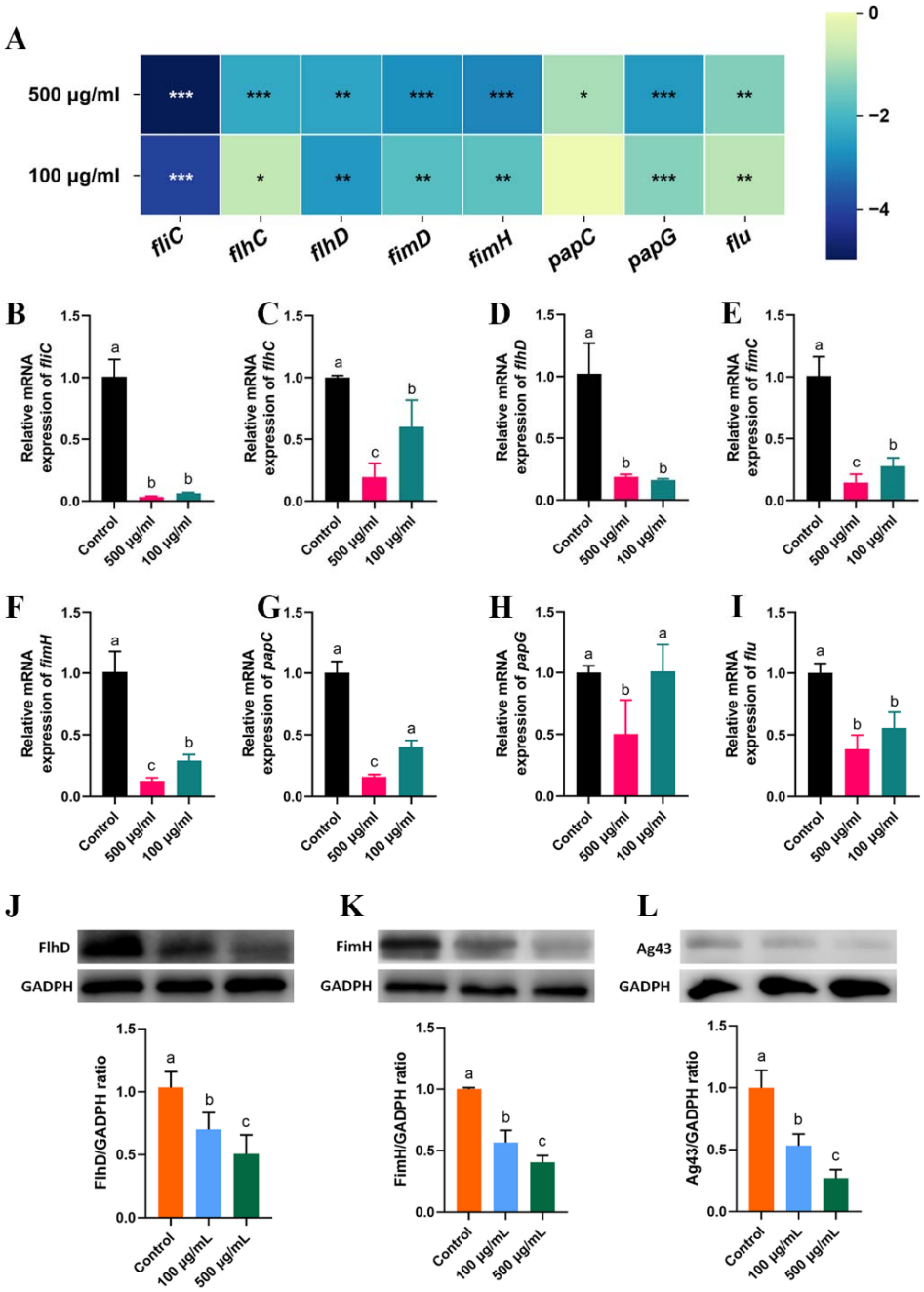

Fig. 5. RT qPCR and Western blot analyses of UPEC virulence associated genes and proteins following PSE treatment. An expression heatmap (A) summarizes the RT qPCR results of virulence associated genes across different treatment groups. The expression levels of individual genes are shown for fliC (B), flhC (C), flhD (D), fimC (E), fimH (F), papC (G), papG (H) and flu (I). Western blot analysis was conducted to determine the protein expression levels of FlhD (J), FimH (K), and Ag43 (L) under the same treatment conditions. Data are presented as mean ± SEM of n = 3 independent experiments. Different superscript letters (a, b, and c) indicate significant differences ($P < 0.05$).

Specifically, PSE treatment significantly reduced the expression of genes related to flagella, including *fliC*, *flhC*, and *flhD*, in a dose dependent manner (Fig. 5B–D). At 1/20 MIC (500 μg/mL), *fliC* expression was reduced by approximately 30-fold compared with the untreated control, and *flhC* and *flhD* were downregulated by approximately 5-fold ($P < 0.05$). At 1/100 MIC (100 μg/mL), *fliC* showed an approximately 16-fold reduction, and *flhC* and *flhD* showed decreases of approximately 2-fold and 6-fold, respectively ($P < 0.05$). Since *fliC* encodes flagellin, the main structural protein of the flagellum, and *flhC* and *flhD* are key components of the FlhDC regulatory complex, these results suggest that PSE not only interferes with flagellar

assembly by inhibiting FliC synthesis but also impairs the regulatory function of FlhDC by downregulating *flhC* and *flhD*. This dual inhibition disrupts UPEC motility and its ability to ascend the urinary tract, thereby reducing its potential to cause ascending urinary tract infections. These findings are consistent with previous studies showing that loss of *fliC*, *flhC*, or *flhD* leads to flagellar loss, impaired motility, and reduced virulence *in vivo* [54-56]. To further confirm the effect of PSE on the flagellar pathway, we performed Western Blot analysis to measure the expression of the representative protein FlhD (Fig. 5J). Quantitative results showed that FlhD expression decreased to 57% and 41% of the control group at 100 μg/mL and 500 μg/mL PSE, respectively ($P < 0.05$). These results validate the inhibitory effect of PSE on the flagellar pathway at the protein level.

Following these findings, we next examined whether PSE affects fimbriae-mediated adhesion and invasion, two key aspects of UPEC virulence. RT-qPCR analysis demonstrated that PSE significantly inhibited the expression of genes involved in UPEC fimbriae biosynthesis and function. Specifically, *fimC* and *fimH*, which are essential for the assembly and adhesion of type 1 fimbriae, were significantly downregulated in a dose dependent manner (Fig. 5E–F). At 500 μg/mL PSE, *fimH* expression was reduced by more than 10-fold, while *fimC* expression decreased by approximately 7-fold compared to the untreated control ($P < 0.05$). Similarly, the *papC* and *papG* genes, which encode key components of P fimbriae, were also significantly downregulated ($P < 0.05$) (Fig. 5G–H). Specifically, *papC* transcription was reduced by approximately 6-fold at 500 μg/mL and by about 2–3 fold at 100 μg/mL ($P < 0.05$), whereas *papG* expression showed a significant decrease of approximately 2-fold only at 500 μg/mL ($P < 0.05$) but not at 100 μg/mL. These molecular changes were consistent with phenotypic observations. TEM images showed a significant reduction in fimbriae on the bacterial surface after PSE treatment. Functional assays further confirmed that PSE significantly inhibited the adhesion and invasion abilities of UPEC strain CFT073. Western Blot analysis showed that FimH, the key adhesin for type 1 fimbriae, was reduced to 70% and 51% of control levels at 100 μg/mL and 500 μg/mL PSE, respectively ($P < 0.05$), confirming the inhibition of fimbrial function at the protein level (Fig. 5K). Fimbriae are critical virulence factors that mediate bacterial adhesion and invasion. Type 1 and P fimbriae play a central role in UPEC urinary tract colonization [57, 58]. FimC, a molecular chaperone, facilitates the proper folding of fimbrial subunits, while FimH, located at the tip of type 1 fimbriae, binds to mannose residues on host cells. PapC forms the outer membrane channel for fimbrial assembly, and PapG serves as an adhesin for host receptor recognition. Loss or mutation of these components significantly impairs UPEC's ability to colonize and invade host tissues [8, 59]. Targeting fimbrial function has therefore emerged as a potential therapeutic strategy. For example, mannose analogs can competitively bind to FimH and significantly reduce bacterial load in bladder infection models [60]. This study supports such strategies, showing that PSE inhibits fimbrial function through downregulation of fimH, fimC, *papC*, and *papG* at both molecular and phenotypic levels. These findings are consistent with recent studies showing that plant-derived compounds targeting fimbrial genes can serve as effective anti-virulence agents [61-63].

In addition to motility and fimbriae-mediated adhesion, biofilm formation is another key virulence factor that allows UPEC to evade host immune responses, resist antibiotics, and establish persistent infections. To assess PSE's effect on this process, we measured the transcription level of the *flu* gene, which encodes antigen 43 (Ag43), a protein involved in bacterial autoaggregation and early biofilm development [64]. High expression of Ag43 is widely regarded as a key marker of biofilm formation in *E. coli* [65]. RT-qPCR results showed that PSE significantly inhibited *flu* gene expression in a dose-dependent manner. At 100 μg/mL and 500 μg/mL, *flu* transcript levels were reduced to 0.56-fold and 0.38-fold of the control group, respectively ($P < 0.05$) (Fig. 5I). This inhibition was confirmed at the phenotypic level by crystal violet staining and fluorescence microscopy, which showed a significant reduction in biofilm biomass after PSE treatment. Furthermore, Western Blot analysis revealed that Ag43 protein expression decreased to 53% and 27% of control levels at the respective concentrations ($P < 0.05$) (Fig. 5L). These results provide molecular evidence for the anti-biofilm activity of PSE and align with previous studies linking *flu* expression to UPEC biofilm formation [9, 66]. Notably, this study is the first to show that PSE interferes with biofilm formation by inhibiting flu gene expression. This adds new evidence supporting the potential of plant polyphenols as biofilm inhibitors [51, 67, 68].

3.7 PSE pretreatment reduces UPEC virulence in a murine UTI model

The ability of UPEC to establish infection in the urinary tract depends not only on its colonization efficiency but also on its capacity to provoke host inflammatory responses that compromise epithelial integrity. In this study, a murine UTI model was established by transurethral instillation of CFT073 strains pretreated with different concentrations of PSE (0, 100, and 500 μg/mL, corresponding to groups M, L_PSE, and H_PSE, respectively). The control group (C) received sterile PBS without bacterial inoculation. The severity of infection was assessed by gross bladder morphology, bacterial burden and inflammatory markers. As shown in Fig. 6A, visual inspection of bladder tissues revealed substantial pathological changes in UPEC-infected mice, including swelling and hyperemia-hallmarks of acute bladder inflammation consistent with previous findings (Hannan et al., 2010). In contrast, these alterations were notably alleviated in PSE-treated groups, particularly at higher concentrations. Histological analysis using H&E staining further validated these observations (Fig. 6B). In the C group, the bladder tissue displayed an intact mucosal layer and muscular layer, with no signs of inflammatory cell infiltration or noticeable pathological changes. In the M group, the bladder tissue showed exfoliation of the urothelial layer and urothelial plaques (red arrow), mucosal atrophy, and infiltration of inflammatory cells in the lamina propria (yellow arrow). Additionally, there was vascular dilation and congestion in the lamina propria (green arrow), indicating significant bladder damage. In the L_PSE group, slight exfoliation of the urothelial layer and urothelial plaques was observed (red arrow), along with mucosal atrophy and a small number of inflammatory cells (yellow arrow). Compared to the model group, the mucosal epithelial shedding and inflammatory cell infiltration were reduced. In the H_PSE group, slight mucosal atrophy was observed, with a few inflammatory cells present (yellow arrow). Compared to the model group, there was a marked reduction in inflammatory cell infiltration, showing significant improvement. Quantitative analysis using the bladder index also support these observations. The index rose

from 0.93 in the C group to 1.43 in the infected model group (M), but decreased to 1.27 and 1.20 in the low and high dose PSE groups (L_PSE and H_PSE), respectively (Fig. 6C). Compared with the model group, both PSE-treated groups showed statistically significant differences ($P < 0.05$).

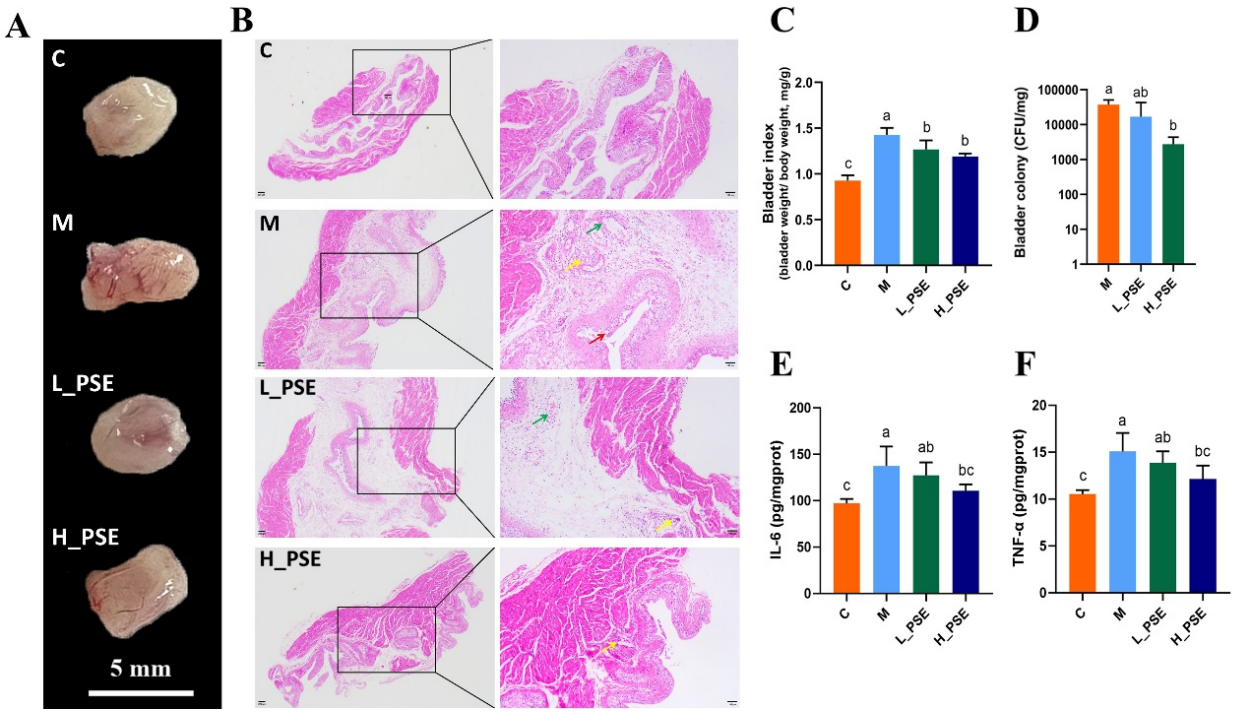

Fig. 6. After PSE intervention, UPEC adhesion and pathogenicity were suppressed. Image of mouse bladders from each group (A) (Scale bar = 5 mm). Image of H&E staining of mouse bladders from each group (B). Bladder index (C), bladder colony count (D), and bladder tissue IL-6 (E) and TNF-α (F) concentrations in each group of mice are shown. Data are presented as mean ± SEM of n = 4 independent experiments. Values with different superscript letters (a, b, and c) were significantly different at $P < 0.05$.

Bladder bacterial burden was also significantly reduced following PSE treatment. While mice in group M harbored an average of 37,356 CFU/bladder, bacterial counts dropped to 16,948 CFU and 2,749 CFU in the L_PSE and H_PSE groups, reflecting 2.2–fold and 13.6–fold reductions, respectively (Fig. 6D). These findings suggest that PSE effectively impairs UPEC colonization of the bladder epithelium and attenuates infection-associated pathological damage *in vivo*. To further assess the inflammatory response, the levels of interleukin-6 (IL-6) and tumor necrosis factor-alpha (TNF-α) in bladder tissues were measured by ELISA and normalized to total protein (pg/mg protein) (Fig. 6E–F). In the M group, IL-6 concentration increased significantly to 137.42 pg/mg protein compared to 97.01 pg/mg in the C group ($P < 0.05$), indicating a marked inflammatory response induced by UPEC infection. PSE pretreatment effectively reduced IL-6 levels to 127.25 pg/mg in the L_PSE group and 110.78 pg/mg in the H_PSE group, corresponding to reductions of 7.4% and 19.4%, respectively, compared to the M group, with statistical significance reached in the H_PSE group ($P < 0.05$). A similar trend was observed for TNF-α. Specifically, TNF-α levels were significantly elevated in the M group (15.09 pg/mg protein) compared with the C group (10.55 pg/mg protein) ($P < 0.05$). PSE pretreatment significantly attenuated this increase, reducing TNF-α concentrations to 13.88 pg/mg and 12.52 pg/mg in the L_PSE and H_PSE groups, respectively, corresponding to decreases of approximately 8.0% and 17.0% relative to the M group, with statistical significance reached in the H_PSE group ($P < 0.05$).

The inflammatory response, a hallmark of UTI pathogenesis, is largely driven by epithelial and immune cell activation in response to bacterial invasion [69]. Infected bladder tissues often exhibit elevated levels of pro-inflammatory cytokines such as IL-6 and TNF-α, which recruit neutrophils to eliminate invading pathogens. However, excessive neutrophil infiltration can also lead to tissue damage and compromise the integrity of the urothelial barrier when inflammation is prolonged [70, 71]. Our findings demonstrated that PSE pretreatment significantly blunted the induction of these cytokines by UPEC. While IL-6 and TNF-α were markedly upregulated in the M group, their levels were dose-dependently reduced in mice infected with PSE-treated bacteria, indicating a less robust activation of the innate immune response. These results not only confirm the weakened inflammatory potential of PSE-modulated UPEC, but also suggest downstream benefits in preserving mucosal integrity and limiting host tissue damage [72]. It should be noted that, in the present study, PSE was only used for in vitro pretreatment of UPEC prior to infection and was not directly exposed to host cells or animals. Therefore, the potential cytotoxicity or systemic safety of PSE toward the host was not specifically evaluated. This experimental design was intended to elucidate the direct regulatory effects of PSE on bacterial virulence, whereas the cytotoxicity toward host cells and *in vivo* safety of PSE as a direct intervention or therapeutic strategy remain to be investigated in future studies.

5. Conclusions

In conclusion, this study demonstrates that PSE, primarily composed of A-type dimers and trimers, significantly attenuate the virulence of UPEC through multiple mechanisms. PSE exhibited dose-dependent antibacterial activity, and more importantly, it impaired key pathogenic traits of UPEC, including motility, adhesion, invasion, type 1 and P fimbriae expression, and biofilm formation. These anti-virulence effects suggest that PSE targets the pathogenic potential of UPEC rather than merely inhibiting its growth. To further assess the *in vivo* relevance of these findings, we used a mouse UTI model in which UPEC pretreated with PSE *in vitro* was directly instilled into the bladder. Mice challenged with PSE-treated UPEC exhibited significantly lower bacterial burdens in bladder tissues and reduced histopathological damage compared to those challenged with untreated bacteria. These results indicate that PSE effectively diminishes the infection severity by suppressing UPEC virulence prior to host exposure, supporting its potential as a novel anti-virulence agent.

Overall, this study highlights the potential of PSE as a natural strategy to mitigate UPEC pathogenicity and prevent UTI. By interfering with critical bacterial virulence mechanisms, PSE may offer a promising adjunct or alternative to conventional antibiotics, especially in the context of rising antimicrobial resistance. Future studies should focus on *in vivo* experiments to evaluate therapeutic dosages, pharmacokinetic profiles, and long-term safety, and to further explore its potential applications in preventive or therapeutic interventions, thereby promoting its clinical translation.

Declaration of competing interest

The authors declare that they have no known competing financial interests or personal relationships that could have appeared to influence the work reported in this paper.

Data availability

No data was used for the research described in the article.

Acknowledgments

This work was supported by the Fundamental Research Funds for the Central Universities (2662025FW012).

References

[1] R. Kyriakides, P. Jones, B.K. Somani, et al., Role of D-mannose in the prevention of recurrent urinary tract infections: evidence from a systematic review of the literature, European Urology Focus. 7 (2021) 1166-1169. https://doi.org/10.1016/j.euf.2020.09.004.

[2] J.J. Carreno, I.M. Tam, J.L. Meyers, et al., Longitudinal, nationwide, cohort study to assess incidence, outcomes, and costs associated with complicated urinary tract infection, Open Forum Infectious Diseases. 6 (2019) ofz446. https://doi.org/10.1093/ofid/ofz446.

[3] M.R. Timm, S.K. Russell, S.J. Hultgren, Urinary tract infections: pathogenesis, host susceptibility and emerging therapeutics, Nat. Rev. Microbiol. (2024) https://doi.org/10.1038/s41579-024-01092-4.

[4] B. Köves, T. Cai, R. Veeratterapillay, et al., Benefits and harms of treatment of asymptomatic bacteriuria: a systematic review and meta-analysis by the european association of urology urological infection guidelines panel, Eur. Urol. 72 (2017) 865-868. https://doi.org/10.1016/j.eururo.2017.07.014.

[5] S. Yamamoto, T. Tsukamoto, A. Terai, et al., Genetic evidence supporting the fecal-perineal-urethral hypothesis in cystitis caused by *Escherichia coli*, The Journal of urology. 157 3 (1997) 1127-1129.

[6] P.A. Schüroff, F.A. Salvador, C.M. Abe, et al., The aggregate-forming pili (AFP) mediates the aggregative adherence of a hybrid-pathogenic *Escherichia coli* (UPEC/EAEC) isolated from a urinary tract infection, Virulence. 12 (2021) 3073-3093. https://doi.org/10.1080/21505594.2021.2007645.

[7] C. Zagaglia, M.G. Ammendolia, L. Maurizi, et al., Urinary tract infections caused by uropathogenic *Escherichia coli* strains-new strategies for an old pathogen, Microorganisms. 10 (2022) 1425. https://doi.org/10.3390/microorganisms10071425.

[8] M.C. Lane, H. Mobley, Role of P-fimbrial-mediated adherence in pyelonephritis and persistence of uropathogenic *Escherichia coli* (UPEC) in the mammalian kidney, Kidney Int. 72 (2007) 19-25.

[9] Z. Naziri, J.A. Kilegolan, M.S. Moezzi, et al., Biofilm formation by uropathogenic *Escherichia coli*: a complicating factor for treatment and recurrence of urinary tract infections, J. Hosp. Infect. 117 (2021) 9-16. https://doi.org/10.1016/j.jhin.2021.08.017.

[10] E.K. Sher, A. Dzidic-Krivic, A. Sesar, et al., Current state and novel outlook on prevention and treatment of rising antibiotic resistance in urinary tract infections, Pharmacol. Ther. 261 (2024) 108688. https://doi.org/10.1016/j.pharmthera.2024.108688.

[11] V.L.T. Tran, E. Hortle, W.J. Britton, et al., Common anti-haemostatic medications increase the severity of systemic infection by uropathogenic *Escherichia coli*, Microbiol. Res. 254 (2022) 126918. https://doi.org/10.1016/j.micres.2021.126918.

[12] R. Sheikhi, M.E. Amini, L. Alidoust, et al., Evaluation of adhesin genes and risk factors associated with urinary tract infections by drug-resistant uropathogenic *Escherichia coli* in North of Iran, Journal of Infection in Developing Countries. 18 (2024) 761-769. https://doi.org/10.3855/jidc.18566.

[13] P. Dawadi, S. Khanal, T. Prasai Joshi, et al., Antibiotic resistance, biofilm formation and sub-inhibitory hydrogen peroxide stimulation in uropathogenic *Escherichia coli*, Microbiology insights. 15 (2022) 11786361221135224. https://doi.org/10.1177/11786361221135224.

[14] M. Xu, C. Lv, H. Wang, et al., Peanut skin extract ameliorates high-fat diet-induced atherosclerosis by regulating lipid metabolism, inflammation reaction and gut microbiota in ApoE$^{-/-}$ mice, Food Res. Int. 154 (2022) 111014. https://doi.org/10.1016/j.foodres.2022.111014.

[15] Daglia. M, .Polyphenols as antimicrobial agents, Curr. Opin. Biotechnol. 23 (2012) 174-181. https://doi.org/10.1016/j.copbio.2011.08.007.

[16] Memar. Y. M, Adibkia. K, Farajnia. S, et al., The grape seed extract: a natural antimicrobial agent against different pathogens, Rev. Med. Microbiol. 30 (2019) 173-182. https://doi.org/10.1097/MRM.0000000000000174.

[17] C. Papuc, G.V. Goran, C.N. Predescu, et al., Plant polyphenols as antioxidant and antibacterial agents for shelf-life extension of meat and meat products: classification, structures, sources, and action mechanisms, Compr. Rev. Food Sci. F. 16 (2017) 1243-1268. https://doi.org/10.1111/1541-4337.12298.

[18] R.C. Allen, R. Popat, S.P. Diggle, et al., Targeting virulence: can we make evolution-proof drugs?, Nat. Rev. Microbiol. 12 (2014) 300-308. https://doi.org/10.1038/nrmicro3232.

[19] S.W. Dickey, G.Y.C. Cheung, M. Otto, Different drugs for bad bugs: antivirulence strategies in the age of antibiotic resistance, Nat. Rev. Drug Discovery. 16 (2017) 457-471. https://doi.org/10.1038/nrd.2017.23.

[20] C.N. Spaulding, R.D. Klein, S. Ruer, et al., Selective depletion of uropathogenic *E. coli* from the gut by a FimH antagonist, Nature. 546 (2017) 528-532.

[21] A.L. Flores-Mireles, J.N. Walker, M. Caparon, et al., Urinary tract infections: epidemiology, mechanisms of infection and treatment options, Nat. Rev. Microbiol. 13 (2015) 269-284. https://doi.org/10.1038/nrmicro3432.

[22] S. Gupta, P. Kumar, B. Rathi, et al., Targeting of *Uropathogenic Escherichia coli papG* gene using CRISPR-dot nanocomplex reduced virulence of UPEC, Scientific Reports. 11 (2021) 17801. https://doi.org/10.1038/s41598-021-97224-4.

[23] C. Roussel, S. Chabaud, J. Lessard-Lord, et al., UPEC colonic-virulence and urovirulence are blunted by proanthocyanidins-rich cranberry extract microbial metabolites in a gut model and a 3D tissue-engineered urothelium, Microbiology Spectrum. (2022) https://doi.org/10.1128/spectrum.02432-21.

[24] A. Howell, J.D. Reed, C.G. Krueger, et al., A-type cranberry proanthocyanidins and uropathogenic bacterial anti-adhesion activity, Phytochemistry. 66 (2005) 2281-2291.

[25] L. Zhao, X.L. Zhu, Y. Yu, et al., Comprehensive analysis of the anti-glycation effect of peanut skin extract, Food Chem. 362 (2021) 130169. https://doi.org/10.1016/j.foodchem.2021.130169.

[26] I. Wiegand, K. Hilpert, R.E.W. Hancock, Agar and broth dilution methods to determine the minimal inhibitory concentration (MIC) of antimicrobial substances, Nat. Protoc. 3 (2008) 163-175. https://doi.org/10.1038/nprot.2007.521.

[27] G. Hidalgo, M. Chan, N. Tufenkji, Inhibition of *Escherichia coli* CFT073 *fliC* expression and motility by cranberry materials, Appl. Environ. Microbiol. 77 (2011) 6852-6857. https://doi.org/10.1128/aem.05561-11.

[28] J. J. Martinez, M. A. Mulvey, J. D. Schilling, J. S. Pinkner, S. J. Hultgren, Type 1 pilus-mediated bacterial invasion of bladder epithelial cells, EMBO J. 19(2000) 2803-2812. https://doi.org/ 10.1093/EMBOJ/19.12.2803.

[29] G.A. O'Toole, L.A. Pratt, P.I. Watnick, et al., Genetic approaches to study of biofilms, Biofilms. 310 (1999) 91-109.

[30] I. Packiavathy, S. Priya, S.K. Pandian, et al., Inhibition of biofilm development of uropathogens by curcumin - An anti-quorum sensing agent from *Curcuma longa*, Food Chem. 148 (2014) 453-460. https://doi.org/10.1016/j.foodchem.2012.08.002.

[31] H. Chia-Suei, D.K. W, H.S. J, A murine model of urinary tract infection, Nat. Protoc. 4 (2009),

[32] R.P. Feliciano, J.J. Meudt, D. Shanmuganayagam, et al., Ratio of "A-type" to "B-type" proanthocyanidin interflavan bonds affects extra-intestinal pathogenic *Escherichia coli* invasion of gut epithelial cells, J. Agric. Food Chem. 62 (2014) 3919-3925. https://doi.org/10.1021/jf403839a.

[33] A. Alejo-Armijo, N. Glibota, M.P. Frias, et al., Synthesis and evaluation of antimicrobial and antibiofilm properties of A-Type procyanidin analogues against resistant bacteria in food, J. Agric. Food Chem. 66 (2018) 2151-2158. https://doi.org/10.1021/acs.jafc.8b00535.

[34] D. Alshaibani, R. Zhang, V.C.H. Wu, Antibacterial characteristics and activity of *Vaccinium macrocarpon* proanthocyanidins against diarrheagenic *Escherichia coli*, J. Funct. Foods. 39 (2017) 133-138. https://doi.org/10.1016/j.jff.2017.10.003.

[35] N.A. Al-Shabib, F.M. Husain, I. Ahmad, et al., Rutin inhibits mono and multi-species biofilm formation by foodborne drug resistant *Escherichia coli* and *Staphylococcus aureus*, Food Control. 79 (2017) 325-332. https://doi.org/10.1016/j.foodcont.2017.03.004.

[36] M.S. Deepika, R. Thangam, P. Sakthidhasan, et al., Combined effect of a natural flavonoid rutin from *Citrus sinensis* and conventional antibiotic gentamicin on *Pseudomonas aeruginosa* biofilm formation, Food Control. 90 (2018) 282-294. https://doi.org/10.1016/j.foodcont.2018.02.044.

[37] X.L. Yang, K.H. Sha, G.Y. Xu, et al., Subinhibitory concentrations of allicin decrease uropathogenic *Escherichia coli* (UPEC) biofilm formation, adhesion ability, and swimming motility, Int. J. Mol. Sci. 17 (2016) 979. https://doi.org/10.3390/ijms17070979.

[38] A. Vikram, G.K. Jayaprakasha, R.M. Uckoo, et al., Inhibition of *Escherichia coli* O157:H7 motility and biofilm by β-Sitosterol glucoside, Biochimica Et Biophysica Acta-General Subjects. 1830 (2013) 5219-5228. https://doi.org/10.1016/j.bbagen.2013.07.022.

[39] J.H. Lee, Y.G. Kim, C.J. Raorane, et al., The anti-biofilm and anti-virulence activities of trans-resveratrol and oxyresveratrol against uropathogenic *Escherichia coli*, Biofouling. 35 (2019) 758-767. https://doi.org/10.1080/08927014.2019.1657418.

[40] J.H. Lee, Y.G. Kim, J. Lee, Carvacrol-rich oregano oil and thymol-rich thyme red oil inhibit biofilm formation and the virulence of uropathogenic *Escherichia coli*, J. Appl. Microbiol. 123 (2017) 1420-1428. https://doi.org/10.1111/jam.13602.

[41] M.C. Lane, C.J. Alteri, S.N. Smith, et al., Expression of flagella is coincident with uropathogenic *Escherichia coli* ascension to the upper urinary tract, Proc. Natl. Acad. Sci. U. S. A. 104 (2007) 16669-16674. https://doi.org/10.1073/pnas.0607898104.

[42] K.T. Hughes, K. Mathee, The anti-sigma factors, Annu. Rev. Microbiol. 52 (1998) 231-286. https://doi.org/10.1146/annurev.micro.52.1.231.

[43] R.M. Yao, X. Mao, Y.L. Xu, et al., Polysaccharides from *Vaccaria segetalis* seeds reduce urinary tract infections by inhibiting the adhesion and invasion abilities of uropathogenic *Escherichia coli*, Front. Cell. Infect. Microbiol. 12 (2022) 1004751. https://doi.org/10.3389/fcimb.2022.1004751.

[44] M.I. Isidro-Coxca, S. Ortiz-Jiménez, J.L. Puente, Type 1 fimbria and P pili: regulatory mechanisms of the prototypical members of the chaperone-usher fimbrial family, Arch. Microbiol. 206 (2024) 373. https://doi.org/10.1007/s00203-024-04092-3.

[45] M.E. Terlizzi, G. Gribaudo, M.E. Maffei, UroPathogenic *Escherichia coli* (UPEC) infections: virulence factors, bladder responses, antibiotic, and non-antibiotic antimicrobial strategies, Frontiers in Microbiology. 8 (2017) 1566. https://doi.org/10.3389/fmicb.2017.01566.

[46] Llano. D. G. D, Roldán. M, Taladrid. D, et al., Cranberry polyphenols and prevention against urinary tract infections: new findings related to the integrity and functionality of intestinal and urinary barriers, J. Agric. Food Chem. 72 (2024) 10328-10338. https://doi.org/10.1021/ACS.JAFC.3C07169.

[47] D. Wojnicz, A.Z. Kucharska, A. Sokół-Letowska, et al., Medicinal plants extracts affect virulence factors expression and biofilm formation by the uropathogenic *Escherichia coli*, Urol. Res. 40 (2012) 683-697. https://doi.org/10.1007/s00240-012-0499-6.

[48] S. Whelan, B. Lucey, K. Finn, Uropathogenic *Escherichia coli* (UPEC)-associated urinary tract infections: the molecular basis for challenges to effective treatment, Microorganisms. 11 (2023) 2169. https://doi.org/10.3390/microorganisms11092169.

[49] W.B. Yang, P. Liu, Y. Chen, et al., Dictamnine Inhibits the Adhesion to and Invasion of Uropathogenic *Escherichia Coli* (UPEC) to Urothelial Cells, Molecules. 27 (2022) 272. https://doi.org/10.3390/molecules27010272.

[50] G.G. Anderson, J.J. Palermo, J.D. Schilling, et al., Intracellular bacterial biofilm-like pods in urinary tract infections, Science. 301 (2003) 105-107. https://doi.org/10.1126/science.1084550.

[51] J.M. Zhang, X. Rui, L. Wang, et al., Polyphenolic extract from *Rosa rugosa* tea inhibits bacterial quorum sensing and biofilm formation, Food Control. 42 (2014) 125-131. https://doi.org/10.1016/j.foodcont.2014.02.001.

[52] C. Rodriguez-Perez, R. Quirantes-Pine, J. Uberos, et al., Antibacterial activity of isolated phenolic compounds from cranberry (*Vaccinium macrocarpon*) against *Escherichia coli,* Food & Function. 7 (2016) 1564-1573. https://doi.org/10.1039/c5fo01441g.

[53] X.F. Shen, L.B. Ren, Y. Teng, et al., Luteolin decreases the attachment, invasion and cytotoxicity of UPEC in bladder epithelial cells and inhibits UPEC biofilm formation, Food Chem. Toxicol. 72 (2014) 204-211. https://doi.org/10.1016/j.fct.2014.07.019.

[54] G.S. Chilcott, K.T. Hughes, Coupling of flagellar gene expression to flagellar assembly in salmonella enterica serovar typhimurium and *Escherichia coli*, Microbiol. Mol. Biol. Rev. 64 (2000) 694-+. https://doi.org/10.1128/mmbr.64.4.694-708.2000.

[55] K.J. Wright, P.C. Seed, S.J. Hultgren, Uropathogenic *Escherichia coli* flagella aid in efficient urinary tract colonization, Infect. Immun. 73 (2005) 7657-7668. https://doi.org/10.1128/iai.73.11.7657-7668.2005.

[56] W.R. Schwan, Flagella allow uropathogenic *Escherichia coli* ascension into murine kidneys, Int. J. Med. Microbiol. 298 (2008) 441-447. https://doi.org/10.1016/j.ijmm.2007.05.009.

[57] H. Remaut, C. Tang, N.S. Henderson, et al., Fiber formation across the bacterial outer membrane by the chaperone/usher pathway, Cell. 133 (2008) 640-652. https://doi.org/10.1016/j.cell.2008.03.033.

[58] K.W. Dodson, J.S. Pinkner, T. Rose, et al., Structural basis of the interaction of the pyelonephritic *E. coli* adhesin to its human kidney receptor, Cell. 105 (2001) 733-743. https://doi.org/10.1016/s0092-8674(01)00388-9.

[59] C.H. Jones, J.S. Pinkner, A.V. Nicholes, et al., FimC is a periplasmic papd-like chaperone that directs assembly of type-1 pili in bacteria, Proc. Natl. Acad. Sci. U. S. A. 90 (1993) 8397-8401. https://doi.org/10.1073/pnas.90.18.8397.

[60] C.N. Spaulding, S.J. Hultgren, Adhesive pili in UTI pathogenesis and drug development, Pathogens. 5 (2016) 30. https://doi.org/10.3390/pathogens5010030.

[61] A.M. Abo-Kamar, A.A. Mustafa, L.A. Al-Madboly, Purified α-Amylase from *Bacillus cereus* exhibits antibiofilm and antiquorum sensing activities against uropathogenic *Escherichia coli*, Downregulating *fimH*, and *papC* virulence genes: implications for urinary tract infections, BMC Microbiol. 24 (2024) 502. https://doi.org/10.1186/s12866-024-03542-8.

[62] N. Foroogh, M. Rezvan, K. Ahmad, et al., Structural and functional characterization of the FimH adhesin of uropathogenic *Escherichia coli* and its novel applications, Microb. Pathog. 161 (2021) 105288. https://doi.org/10.1016/j.micpath.2021.105288.

[63] X. Mao, H.L. Guo, R.M. Yao, et al., Crude polysaccharides from the seeds of *Vaccaria segetalis* prevent the urinary tract infection through the stimulation of kidney innate immunity, J. Ethnopharmacol. 260 (2020) 112578. https://doi.org/10.1016/j.jep.2020.112578.

[64] M.W. van der Woude, I.R. Henderson, Regulation and function of Ag43 (Flu), Annu. Rev. Microbiol. 62 (2008) 153-169. https://doi.org/10.1146/annurev.micro.62.081307.162938.

[65] B. Zalewska-Piatek, R. Piatek, M. Olszewski, et al., Identification of antigen Ag43 in uropathogenic *Escherichia coli* Dr^+ strains and defining its role in the pathogenesis of urinary tract infections, Microbiology-Sgm. 161 (2015) 1034-1049. https://doi.org/10.1099/mic.0.000072.

[66] M.A. Schembri, K. Kjærgaard, P. Klemm, Global gene expression in *Escherichia coli* biofilms, Mol. Microbiol. 48 (2003) 253-267. https://doi.org/10.1046/j.1365-2958.2003.03432.x.

[67] I. Goto, S. Saga, M. Ichitani, et al., Investigation of components in roasted green tea that inhibit *Streptococcus mutans* biofilm formation, Foods. 12 (2023) 2502. https://doi.org/10.3390/foods12132502.

[68] H.S. Cho, J.H. Lee, S.Y. Ryu, et al., Inhibition of pseudomonas aeruginosa and *Escherichia coli* O157:H7 biofilm formation by plant metabolite ε-viniferin, J. Agric. Food Chem. 61 (2013) 7120-7126. https://doi.org/10.1021/jf4009313.

[69] S.N. Abraham, Y.X. Miao, The nature of immune responses to urinary tract infections, Nat. Rev. Immunol. 15 (2015) 655-663. https://doi.org/10.1038/nri3887.

[70] D. Martin-Sanchez, M. Fontecha-Barriuso, M.D. Sanchez-Niño, et al., Cell death-based approaches in treatment of the urinary tract-associated diseases: a fight for survival in the killing fields, Cell Death Dis. 9 (2018) 118. https://doi.org/10.1038/s41419-017-0043-2.

[71] D. Butler, I. Ambite, M.L.Y. Wan, et al., Immunomodulation therapy offers new molecular strategies to treat UTI, Nature Reviews Urology. 19 (2022) 419-437. https://doi.org/10.1038/s41585-022-00602-4.

[72] T.J. Hannan, I.U. Mysorekar, C.S. Hung, et al., Early severe inflammatory responses to uropathogenic *E-coli* predispose to chronic and recurrent urinary tract infection, PLoS Pathog. 6 (2010) e1001042. https://doi.org/10.1371/journal.ppat.1001042.